Building Simulation 2003

Eighth International IBPSA Conference
Eindhoven, Netherlands
August 11-14, 2003

HEAT FLUX MEASUREMENT OF URBAN BOUNDARY LAYERS IN KYOTO CITY AND ITS PREDICTION BY CFD SIMULATION

Kazuya Takahashi[1], Harunori Yoshida[2], Yuzo Tanaka[3],
Noriko Aotake[1] and Fulin Wang[1]

[1]Graduate Student, Dept. of Urban and Environmental Eng., Faculty of Eng., Kyoto University
[2]Prof., Dept. of Urban and Environmental Eng., Faculty of Eng., Kyoto University, Dr.Eng.
[3]Yamatake Corporation, M.Eng.

ABSTRACT

In the summer of 2002, measurements were simultaneously performed to investigate the characteristics of heat flow in urban areas at three locations in Kyoto city: 1) a commercial urban area mixed with low-rise traditional residential buildings that represents the urban area of Kyoto, 2) an university campus area with a lot of green zones, and 3) a plaza covered with a concrete slab which was used as a reference point of measurement. Heat flux of boundary layer over the three locations and the surface temperatures of building walls and streets were measured to investigate the urban thermal environment. For the analysis, a new simulation code was developed by combining unsteady state heat conduction of building walls and grounds, radiation heat exchange between them, and airflow by CFD (Computational Fluid Dynamics). By using this code, the thermal environment of the urban areas such as air temperature, humidity, wind velocity, and boundary layer heat flux was predicted and compared with the measured results. It was found that this model could predict the real thermal environment of the urban area. Using this code, the effect of additional green on roofs and grounds can be investigated in order to mitigate urban heat island and to improve urban thermal environment at the street level.

INTRODUCTION

It is a well-known fact that the urban air temperature is gradually rising in all cities and some effective measures are needed to mitigate it. Several factors are reported to be the cause of the temperature rise, such as diminishing of green area, low wind velocity due to high building density and change of street surface coating materials. However urban planning based on the prediction of urban environment incorporating the effects of these factors is under development (Williamson et al., 2001).

A lot of researches have been performed on the measurement and the analysis of urban environment, however, there are few researches that compare measured and simulated heat flux over urban areas and simultaneously measured thermal environments of several areas with different topographical features. Such comparative measurement and simulation method enable the analysis of the factors that influence the urban environment. In addition there are many researches regarding urban thermal environment simulation, however, there are few researches in predicting it by combining 3-dimensional CFD simulation model and unsteady state heat conduction of building walls and grounds. Moreover few of them compared the simulated results with the measured results and verified simulation accuracy (Harayama et al., 2002).

The purpose of this research is: 1) to clarify the influence of local topological features on urban temperature and humidity: 2) to compare sensible and latent heat flux characteristics of the urban areas with different amount of built and green area: and 3) to predict urban thermal environment by developing a new numerical simulation model combining air flow and temperature calculation by CFD and transient heat conduction calculation of buildings and grounds.

MEASUREMENT OF HEAT FLUX, TEMPERATURE AND HUMIDITY

We measured the sensible heat flux and the latent heat flux transported from the urban surface to the upper atmosphere, and the temperature of buildings' walls and streets at three typical sites. The first site is a central part of Kyoto city (Site U) which is bristling with medium height commercial buildings mainly. The second site is a university campus (Site C) with much greenery such as a green court, and a hill covered with ample green, called Mt. Yoshida Yama, is closely located eastward. The third site is a city-hall plaza (Site R) covered with concrete pavement and is used as a reference measuring site for the present and future analysis.

Turbulent sensible and latent heat fluxes were calculated based on eddy correlation method, namely by the following equations (Tukamoto et al.,).

$$H = \overline{\rho C_p w' T'} \quad (1)$$

$$\ell E = L\overline{w' \rho q'} \quad (2)$$

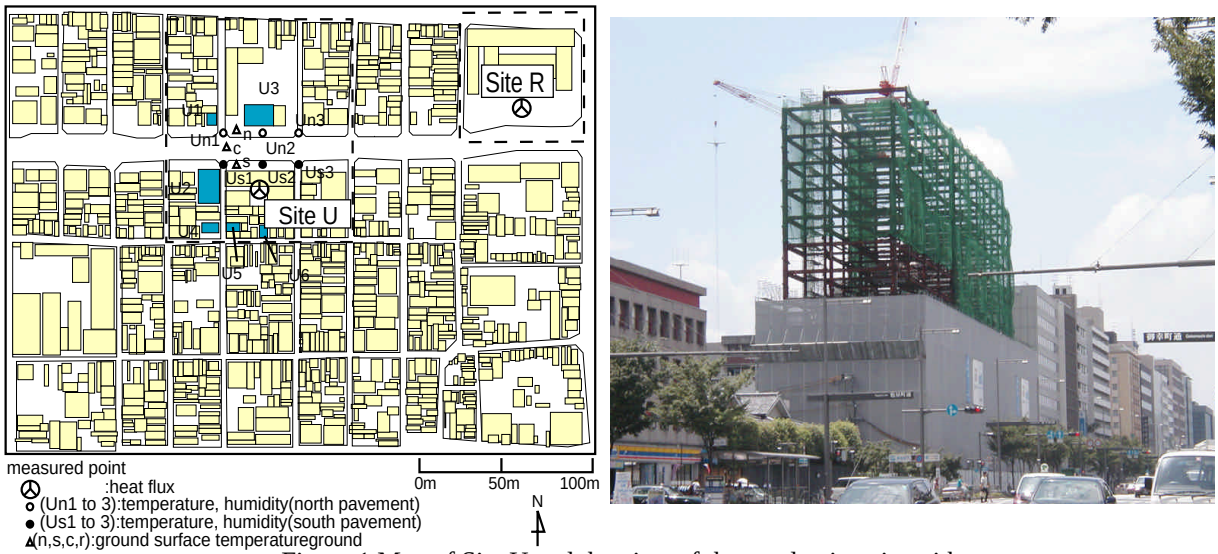

Figure 1 Map of Site U and the view of the conduction site with a crane

Figure 2 Map of Site C and the view of the campus courtyard

The wind velocity fluctuation w' and temperature fluctuation T' were measured by a three-dimensional ultrasonic anemometer and humidity fluctuation q' by an infrared absorption hygrometer. These values are defined as the fluctuations around the average value of each variable, which was obtained by averaging recorded data of 60 minutes.

The measuring instruments were hanged by a crane raised on a building construction site. Atmospheric temperature and humidity inside the sites were measured at the height of 1.5m and the surface temperature of building walls and streets were measured by a handy radiometric thermometer. Both measurements were carried out manually by moving around the sites.

The measurements were conducted from 10:00 to16:00 on July 21st and 28th, 2002. The measurement points of Site U and Site R are shown in Figure 1, the measurement points of Site C are shown in Figure 2.

Heat flux

Each site's heat flux of July 21st and July 28th are shown in Figure 3 and 4. On both days, the sensible heat flux H of Site U is 150 to 300W/m^2 and it is about 40% to 50% of the net radiation. The latent heat flux ℓE of Site U is within the range of -50 to 50W/m^2 and its average is approximately zero. We define the ground surface heat flux $G = Rn - H - \ell E$, which is the result of net radiation Rn subtracted by sensible heat flux H and latent heat flux ℓE . G is about 40% to 60% of the net radiation Rn in any period.

With respect to Site C, the sensible heat H is about 100 to 150W/m^2 on July 21st when the net radiation Rn is small and about 150 to 200W/m^2 on July 28th when the net radiation Rn is large. The sensible heat flux H of Site C is about 30% of the net radiation Rn of each day, and is about 50 to 100W/m^2 smaller than that of Site U. The latent heat flux ℓE of Site C is 50 to

150W/m^2 and is about 100W/m^2 larger than that of Site U. The reason for these phenomena can be the influence of the greens surrounding Site C and this assumption will be validated by CFD simulation later in section 3.

The ratio of H, ℓE and G on July 21st and July 28th to the net radiation Rn from 10:00 to 16:00 is shown in Figure 5 and Figure 6. The ratio of turbulent heat flux, which is the sum of H and ℓE , to the net radiation Rn of Site U and Site C is about 50% on both days. The turbulent heat flux ratio of Site R is about 20%, which is much smaller than that of Site U and Site C. The ratio of latent heat flux to the net radiation of Site C is about 20%, and the latent heat flux ratio of Site U and Site R are about zero. Thus, we can conclude from the measurement that the reason for little latent heat flux on Site U and Site R is due to less green.

Temperature distribution

Figure 7 and 8 show the average air temperature of several measurement points, which are 1.5m above the ground of Site U and Site C, on July 21st and 28th. In addition the average values of these temperatures from 10:00 to 16:00 are also shown in these figures. We defined T_u as the average air temperature of six measurement points on Site U, $T_{c,g}$ as the average temperature of points Cg1 to Cg4 on the part of Site C that are close to courtyard trees, and $T_{c,n}$ as the average temperature of points Cn1 to Cn6 on the part of Site C that are apart from the trees. The average $T_{c,n}$ from 10:00 to 16:00 is 0.2ºC lower than that of T_u on July 21st and is 0.9ºC lower than that of T_u on July 28th. The temperature difference is greater on July 21st than that on 28th. The wind on July 21st was from the south where no much green area exists and on July 28th it was from the east where the green hill exists. Therefore the influence of green area on July 28th is greater than that on July 21st and this might be the reason of the difference. The average of $T_{c,g}$ from 10:00 to 16:00 is smaller than that of T_u on both days, and the temperature difference is similar for both days. The reason of this similarity can be due to the assumption that green area dominates the temperature close to itself.

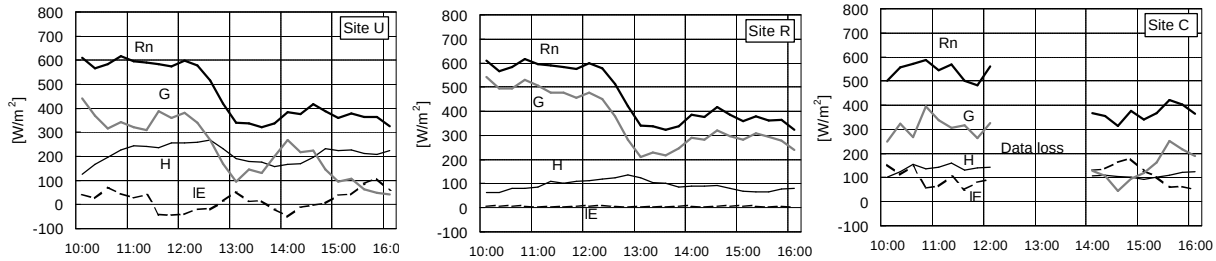

Figure 3 Heat flux components (July 21)

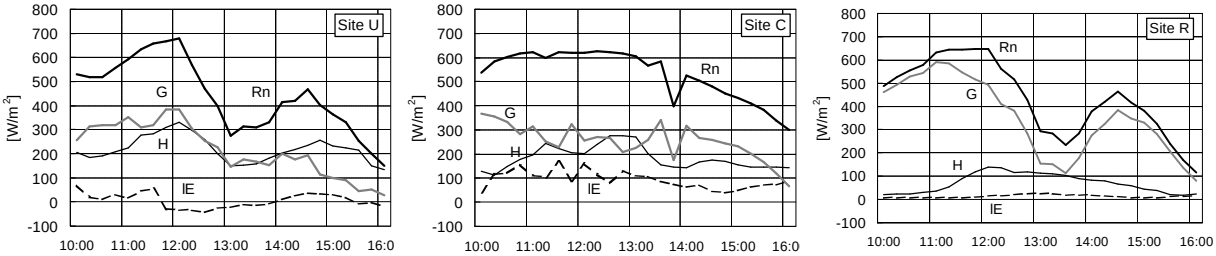

Figure 4 Heat flux components (July 28)

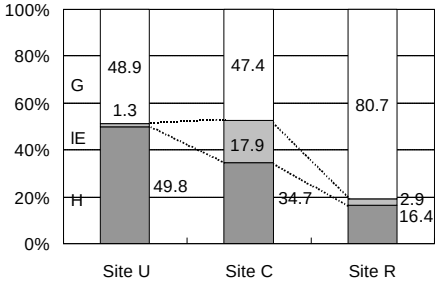

Figure 5 Average ratio of heat flux components to net radiation (July 21)

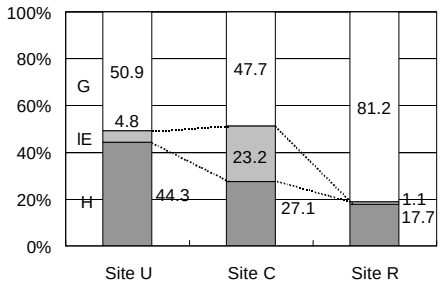

Figure 6 Average ratio of heat flux components to net radiation (July 28)

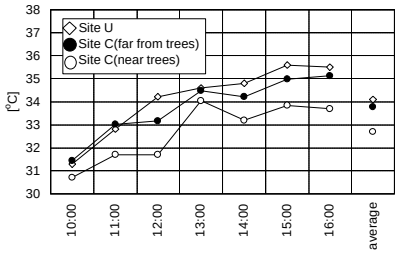

Figure 7 Air temperatures of Site U and C (July 21)

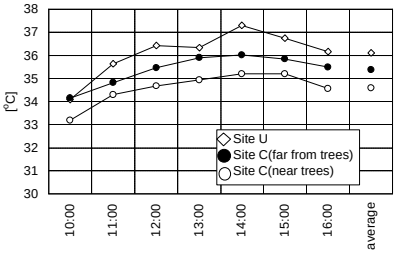

Figure 8 Air temperatures of Site U and C (July 28)

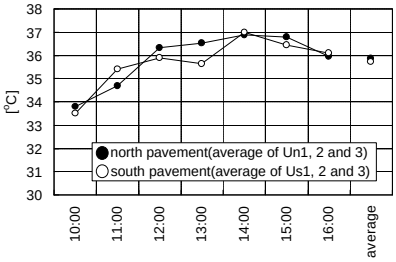

Figure 9 Air temperatures on pavement (July 28)

Figure 9 shows the average air temperature of north and south side of pavement on Site U. (The north side temperature is the average of point Un1 to 3 and the south side is the average of point Us1 to 3.) The north side receives the sunshine and the south is in the shade. However, the maximum air temperature difference of these two temperatures is only 1ºC. The reason can be that this main street is wide and open to the sky and air of both sides is mixed easily within the urban canyon and with the upper atmosphere as well. In section 3 we will verify whether these hypotheses are verified or not by CFD simulation.

CFD SIMULATION

In this section, we predict heat flux and distribution of air temperature and humidity of Site U and Site C using CFD simulation and using measured surface temperature as boundary conditions. Configurations and sizes of urban buildings are modeled similar to the real ones as much as possible. The calculation results were compared with the measurement results and the simulation accuracy was checked.

Models

This CFD simulation uses the *k-e* three-dimensional turbulent flow model improved by Launder and Kato.

$$r = const. \tag{3}$$

$$\frac{\partial u_i}{\partial x_i} = 0 \tag{4}$$

$$\frac{\partial r u_i}{\partial t} + \frac{\partial r \overline{u_j} \overline{u_i}}{\partial x_j} = -\frac{\partial P}{\partial x_i} + \frac{\partial}{\partial x_j} m \frac{\partial u_i}{\partial x_j} - r g_i (T - T_o) \tag{5}$$

$$\frac{\partial r C_p T}{\partial t} + \frac{\partial u_i C_p T}{\partial x_j} = \frac{\partial}{\partial x_j} K \frac{\partial T}{\partial x_j} + \dot{q} \tag{6}$$

We assume the fluid to be incompressible (equation-3), and solve the simultaneous equations of conservation laws of mass (equation-4), momentum (equation-5), and energy (equation-6). We make pressure correction using the SIMPLE method.

We evaluate generation of water vapor *E* due to transpiration by trees on Site C (equation-7), which is the shaded part of Figure 2 and with a green hill in the east (not shown). The heat absorption by trees' transpiration is calculated by the equation (8) (Yoshida, S. et al.,).

$$E = aV_n E_s = aV_n b a_w (f_a - f_s) \tag{7}$$

$$\ell E = LE \tag{8}$$

The leaf area density is taken as the average of keyaki (a Japanese tree) and camphor tree.

Moreover, air resistance by trees is also evaluated by adding the term (9) to the momentum equation (5) and turbulence generation and dissipation by trees by adding the term (10) and (11) to the *k* and *e* equation respectively.

$$-hC_d a u_i^2 / 2 \tag{9}$$

$$\frac{e}{k} hC_d a u_j^3 \tag{10}$$

$$hC_d a u_j^3 \tag{11}$$

Boundary conditions

Inflow conditions to the simulation area were generated as shown in Figure 10. Firstly, a 120m long standard urban district block is made based on the urban characteristic which represents the windward urban area for the simulation area. Then ten such standard blocks were cyclically connected to form a

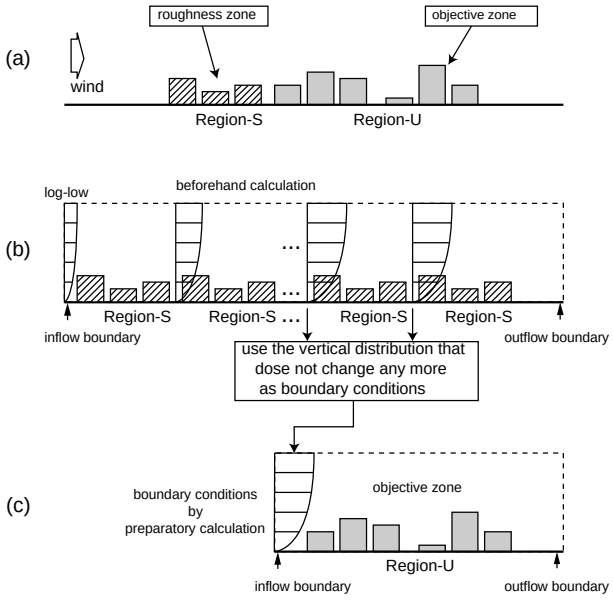

Figure 10 Method to obtain inflow boundary conditions

large uniform urban area. The assumption of law of exponent in vertical distribution of horizontal wind velocity and turbulent energy was applied to the inflow of the model. We define this as S-condition.
After checking that how much change occurred in vertical distributions of horizontal velocity, air temperature and turbulent energy along the flow direction, we found these vertical distributions became almost constant after air passed through eight blocks. Therefore we adopted these distributions as the inflow boundary conditions for the simulation model. Figure 11 shows these conditions obtained.

The green hill is situated 200 meters east of the measurement point on Site C. Between the measurement point and the green area there is a residential building zone. We define this as Case-1.

As a comparison two cases were simulated. Namely Case-2 is 50% less green area than Case-1 and Case-3 is no green area. For these cases the inflow condition-S was applied.

The dissipation ratio in turbulence was calculated using Equation (12). This is derived based on the assumption that generated and dissipated turbulences are balanced at the inflow boundary. The boundary condition of log-law was applied in calculating stress on surfaces. The top and side of simulation area was assumed having a free-slip boundary. The heat transfer coefficient on surfaces was taken to be 11.6 W/m^2. The air temperature on the top of the analytical area was fixed at the temperature measured by Kyoto Meteorological Department.

$$e(z) = C_t^{0.5} k(z) \frac{U_s}{z_z} a \left(\frac{z}{z_z} \right)^{(a-1)} \tag{12}$$

Calculation of heat flux

In CFD simulation sensible and latent heat flux was evaluated by the following equations (Murakami, S.).

$$H = -\overline{r C_p w'T'} = K_t \frac{\partial T}{\partial z} \tag{13}$$

$$K_t = \frac{m_t C_p}{P_{rt}} \tag{14}$$

$$m_t = C_t r \frac{k^2}{e} \tag{15}$$

$$\ell E = -Lba_w (f_a - f_s) = L r D_{mt} \frac{\partial C}{\partial z} \tag{16}$$

$$D_{mt} = \frac{m_t}{r S_{ct}} \tag{17}$$

Simulation results

The simulation was performed only for the time of 12:00 on July 28th and the results were investigated. The surface temperatures measured on the building walls and grounds are shown in Table 1 and 2. The

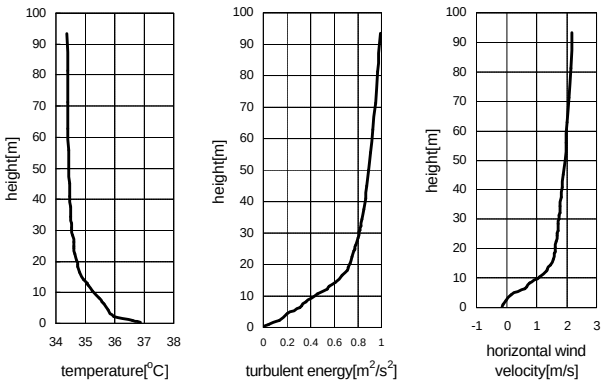

Figure 11 Inflow boundary conditions

simulation results of the air temperature of Site U are shown in Table 3. The average difference between measurements and calculation (measurement values are subtracted from simulation values) is +0.9ºC. The average difference among the locations where both sunshine and shade appear (Us1 to Us 3) is +1.6ºC and this is greater than that (+0.3ºC) of the locations where only sunshine appears (Un1 to Un 3). The simulated air temperature at the height of 45m above the ground is 34.6ºC. This is exactly the same as the measured value. These results demonstrate that the air temperature influenced by the heat exhausted from buildings and the ground surfaces can be estimated well by CFD.

The simulation results of heat flux of Site U are shown in Table 4. The simulated sensible heat flux is 197W/m^2, however, the measured is 329 W/m^2. The

Table 1 Wall and ground surface temperature of Site U

	surface temperature[°C]	mesured point
north wall	36.4	north wall of U2
south wall	42.6	south wall of U1, U3, U5, U6
west wall	37.6	west wall of U4
east wall	37.7	east wall of U2
ground(alley)	57.7	t
ground(south pavement)	46.3	s
ground(north pavement)	61.4	n
roof	60.5	p

Table 2 Wall and ground surface temperature of Site C

	surface temperature[°C]	mesured point
north wall	36.8	north wall of C
south wall	41.4	south wall of C
west wall	42.6	west wall of C
east wall	35.5	east wall of C
ground	52.2	average of Cn1 to 6 and Cg1 to 4
roof	45.2	average of Cn1 to 6 and Cg1 to 4

Table 3 Temperatures of Site U
M - Measurement; S - Simulation.

	Un1	Un2	Un3	Us1	Us2	Us3	average
Site U(M)	36.6	35.9	36.5	34.0	36.1	35.7	35.8
Site U(S)	36.6	36.7	36.4	37.5	36.4	36.8	36.7
difference	0	+0.8	-0.1	+3.5	+0.3	+1.1	+0.9

Table 4 Heat flux of Site U at the height of 45m
M - Measurement; S - Simulation.

	sensible heat flux H[W/m^2]	turbulent energy k[m^2/s^2]
Site U (M)	329	1.02
Site U (S)	197	0.80

simulation result is about 40% less than the measured value. In Figure 12 the distribution of sensible heat flux at the height of 45 m is shown. We can see quite much difference exists and this is due to complex urban building configurations. In our calculation the building being under construction was modeled as a structure formed by steel beams and columns, however, this structure may cause more effect on air flow than simulated. This problem will be further investigated in future.

The simulated air temperatures of Case-1 (Site C), Case-2 (50% less green area), and Case-3 (no green area) are shown in Table 5. In Case-1, the difference between simulated and measured temperature of the locations being apart from the trees (Cn1 to Cn6) is +0.5ºC, and that of the locations which are close to the trees (Cg1 to Cg4) is -0.8ºC. The average temperature of the points being apart from trees (Cn1 to Cn6) of Case-2 is 0.2ºC higher than that of Case-1 and for Case-3 it is 0.4ºC higher than Case-1. These results show that the air temperature of the points being apart from trees (Cn1 to Cn6) is lowered with the increase of green area in the direction of windward. This agrees with the measurement results previously shown.

SIMULATION COMBINING RADIATION, CONDUCTION AND CFD

The measured surface temperatures of buildings and ground were used for CFD simulation mentioned in the former section. Since no surface temperature is available for predicting environment of a given urban area, we have developed a new simulation code which can simulate it by combining CFD calculation with surface radiation exchange calculation and unsteady state heat transfer calculation of buildings' walls and grounds. Calculation procedures are as follows (Figure 13).

1) Initial temperature: Calculating initial surface temperatures on the basis of unsteady state heat transfer by giving 30 days meteorological data of air temperature, solar radiation and long-wave radiation. This implies that air temperature distributions in the urban space and radiation exchange are neglected in surface temperature calculation.

2) Condition setting at time j: Providing meteorological data at time j and evaluating the surface temperatures based on at time j-1 as initial condition.

3) Radiation exchange between surfaces: Calculating heat absorbed at each surface element considering mutual reflection of direct sunbeam and sky radiation, and long wave radiation between all the surfaces. The short wave absorptivity of a wind pane is set 0.9, and 0.2 for wall and ground surfaces. The average absorptivity was calculated by assuming the ratio of

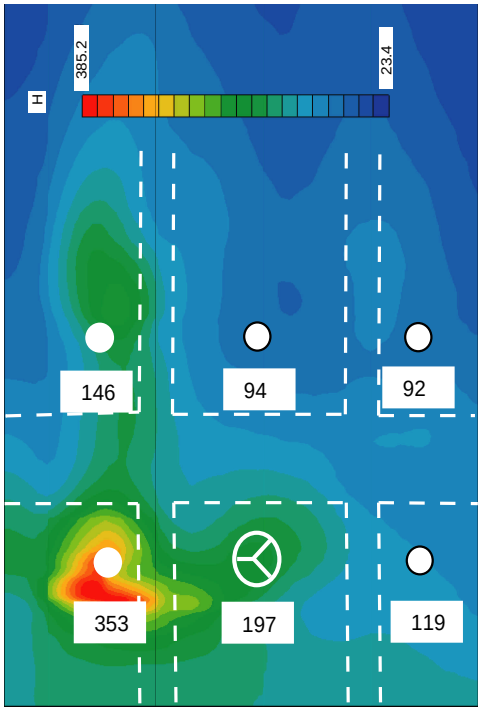

Figure 12 The distribution of sensible heat flux at the height of 45 m [W/m^2]

Table 5 Temperatures of Site C
M - Measurement; S - Simulation.

	average of Cn	average of Cg	atmosphere(h=45m)
Site C(M)	35.8	35.0	34.1
Site C(S)	36.3	34.2	34.7
difference (S-M)	+0.5	-0.8	+0.6
green area 50%	36.5	34.1	34.9
no green area	36.7	34.5	35.2

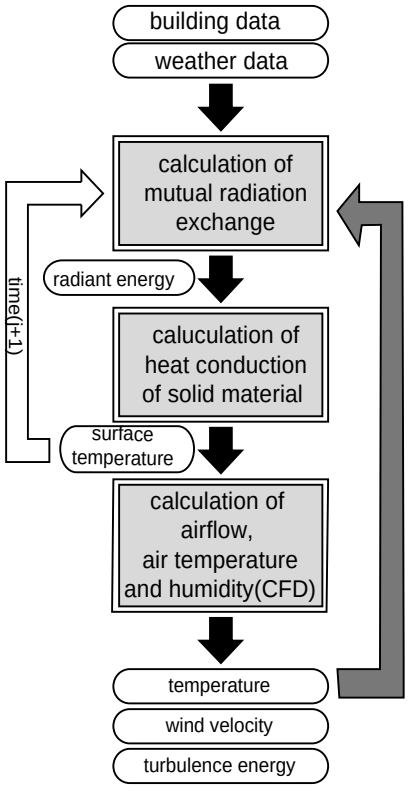

Figure 13 Calculation of heat conduction

the pane and wall surface area is 0.2 : 0.8. Long wave absorptivity is set 0.9.

4) Unsteady state heat transfer: Calculating or updating the temperatures of wall and ground at time J+1 by solving the 1-dimenssional unsteady state heat conduction equation.

5) Calculation process: Proceeding steps from 2) to 4) at every one minute and air temperature is updated by performing CFD calculation every 60 minutes.

Simulation case

The date and the place for the simulation is from 10 to 16 o'clock on July 28th at Site U. Buildings' walls are composed of mortar (12.5mm), normal concrete (225mm), and mortar (12.5mm). The room air temperature is conditioned to be 26 °C. The ground is composed of asphalt (50mm), gravel (150mm), and soil (800mm). The bottom side of the ground was assumed to be thermally insulated.

Discussion of calculation results

Figure 15 shows the surface temperatures of the walls and the ground. The average difference between simulated and measured temperature of east walls is +0.2°C and the average (simulated - measured) difference of all direction walls is -0.4°C. The maximum difference between simulated and measured temperature of the ground surface is 10.7°C and the average difference of all the measurement points is 2.1°C.

Figure 16 shows the simulation results of urban air temperature. The difference between the simulated and the measured air temperature is from -0.8°C to +3.5°C and the average is 0.5°C. Since the measurement point Us1 has lower measured temperature than other points, large difference ranging from +0.7°C to +3.5°C exists. The difference of other measurement points is from +0.8°C to +1.0°C and the average is +0.3°C.

As mentioned above the simulation results agree with the measured values quite well. This means that this simulation can be used as a tool to analyze the influence of building shapes and urban configurations on urban heat island and to improve the urban environment by predicting the effect of various urban designs or feasible modifications.

CONCLUSIONS

Intensive measurement of urban environment was performed including air temperature, surface temperature of building walls and streets, solar radiation, long-wave radiation, sensible heat flux and latent heat flux, and the results were compared with simulation results. We can summarize the conclusions as follows.

1) The results of urban environment measurement of a central city without much green and an university campus with enough green show the existence of distinct air temperature difference between these two sites. The difference can be well predicted by CFD simulation, however, measured heat flux at the height of 45m is 40% larger than the estimated. One reason of this discrepancy may be due to too much simplification in modeling the building situated in the measurement site, but this must be investigated further in our future work.

2) To predict the environment formed by an urban design or renovation a new simulation code

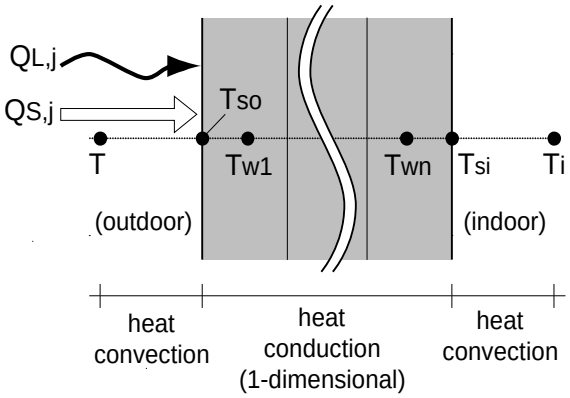

Figure 14 Calculation method of unsteady state heat conduction

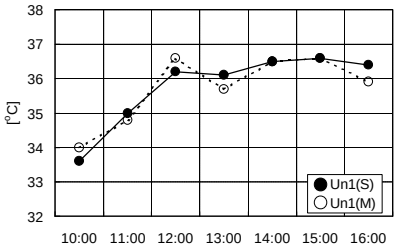

Figure 16 Simulation results of air temperature of Site C

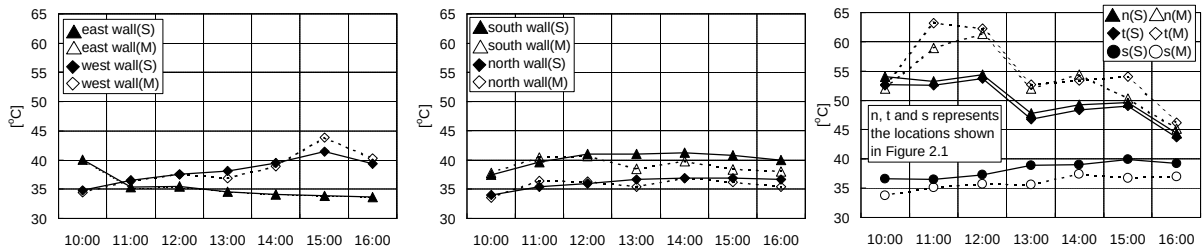

Figure 15 Simulation results of wall and ground surface temperature

combining CFD simulation, radiation exchange between surfaces and unsteady state heat conduction of buildings and the ground was developed. As good agreement between the measured and predicted air temperatures by this code was obtained, this simulation code can be a tool for urban design and renovation.

In the present investigation heat generated by human activity or anthropogenic heat was not considered. Although it is not large in the present city because most buildings are low rise even in the city center and mobile traffic is not heavy, we are planning to include and analyze its effect in our future work.

NOMENCLATURE

a : Leaf area density [m^2/m^3](=0.39m^2/m^3)
a_w :Coefficient of humidity conduction [kg/m^2skPa]
b : Evaporative efficiency [-]
C : Humidity ratio [kg/kg(DA)]
C_d : Resistance coefficient of the crowns of trees [-](=0.5)
C_p : Specific heat of air [J/kgK]
C_t : Model constant [-](=0.09)
D_{mt} : Coefficient of turbulence diffusion[m^2/s]
E_s : Steam amount from leaves transpiration [kg/m^2s]
f_a : Partial pressure of steam [kPa]
f_s : Saturation partial pressure of steam [kPa]
g_i : Acceleration [m/s^2]
G : The ground surface heat flux[W/m^2]
k : Turbulent energy [m^2/s^2]
K : Coefficient of heat conduction [J/msK]
L : Latent heat of vaporization (=2.5×10^6 [J/kg])
P : Air pressure [N/m^2]
P_{rt} : Prandtl number of turbulence[-](=0.9)
q : Heat generation [J/m^3s]
S_{ct} : Schmidt number of turbulence[-] (=0.9)
t : Time [sec]
T : Air temperature [K]
T_0 : Basic air temperature [K](=303)
u_i : Velocity [m/s]
U_s : Wind velocity on reference height [m/s]
V_n : Volume of the crown of trees [m^3]
x_i : Space co-ordinate [m]
a : Exponential order[-](=0.2)
b : Coefficient of volume expansion [l/K]
e : Dissipation rate of turbulence energy [m^2/s^3]
h : The ratio of the crowns of trees [-]
m : Coefficient of viscosity [kg/ms]
m_t : Coefficient of eddy viscosity[kg/ms]
r : Density of air [kg/m^3](=1.176)

REFERENCES

Harayama, K. and S. Yosida: Numerical study based on unsteady radiation and conduction analysis, Prediction of outdoor environment with unsteady coupled simulation of convection, radiation and conduction -Part 1-, J. Archit. Plann. Environ. Eng., AIJ, No. 556, 99-106, June 2002

Murakami, S. et al.,: Computational Environment Design for Indoor and Outdoor Climates, University of Tokyo Press, 2000

Tukamoto, O. et al.,: Meteorological study note No.199, 2001, Meteorological Society of Japan

Tanimoto, J. and T. Katayama: A study on turbulent flux in an urban and rural area based on a field measurement, J. Archit. Plann. Environ. Eng., AIJ, No. 513, 69-76, November 1998

Williamson, T. J. and Evyatar Erell: Thermal performance simulation and the urban microclimate: measurement and prediction, Seventh Internal IBPSA Conference, Rio de Janeiro, Brazil, August 13-15, 2001

Yoshida, S.: Study on effect of greening on outdoor thermal environment using three dimensional plant canopy model, J. Archit. Plann. Environ. Eng., AIJ, No. 536, 87-94, Oct., 2000